

Gold nanorod distribution in mouse tissues after intravenous injection monitored with optoacoustic tomography

Richard Su, Anton V. Liopo, Hans-Peter Brecht, Sergey A. Ermilov and Alexander A. Oraevsky

TomoWave Laboratories Inc. 675 Bering Dr., Suite 575, Houston, TX 77057
www.tomowave.com

ABSTRACT

We used a three-dimensional optical tomography system that was previously developed to create high contrast maps of optical absorbance of mice tissues. In this study, animals were scanned before and after injection of gold nanorods (GNRs) at different time periods. As-synthesized GNRs were purified from hexadecyltrimethylammonium bromide (CTAB) and coated with polyethylene glycol (PEG) to obtain GNR-PEG complexes suitable for *in vivo* applications. Intravenous administration of the purified GNR-PEG complexes to mice resulted in an enhanced contrast of normal tissues and blood vessels as compared to ordinary nude mice. In parallel with optoacoustic imaging we investigated the accumulation of GNRs in liver using invasive analytical techniques. Maximum levels of GNRs in liver macrophages were observed after 48-72 hours post-injection, followed by slow clearance trend after 8 days. Optoacoustic imaging revealed redistribution of GNR in mouse organ and tissues: in the initial hours, accumulation of GNRs is seen predominantly in the periphery of the mouse, while a gradual increase of GNR levels in liver, spleen and kidneys is seen in 1 and 24 hours.

Keywords: optoacoustic, gold nanorods, 3D tomography, nude mice, kidneys, liver, spleen, silver staining

1. INTRODUCTION

Nanotechnology offers new means towards developing novel and efficient methods and drugs for treatment of cancer. Methods of enhancing contrast of optoacoustic images with strongly absorbing gold nanoparticles have been first discussed a decade ago.¹ Indeed, gold nanoparticles (GNPs) have minute sizes and sufficiently large surface area so that they can easily penetrate cellular membranes and deliver high payloads of targeting agents and cancer-killing drugs to achieve specificity and improved therapeutic potential. Moreover, being exceptional absorbers for different types of energy radiation GNPs themselves may serve as therapeutic agents for cancer therapy.² One prevalent nanoparticle with a strong plasmon resonance in the near-infrared spectral range is gold nanorods (GNR) and its peaks in the near-infrared region.³ Despite their large potential, nanoparticles present inherent risks and challenges. Although *in vitro* and short-term *in vivo* studies have demonstrated the absence of toxicity for different types of gold nanoparticles, the legitimate concerns related to their potential long-term toxicity and relatively slow clearance rates remain poorly addressed. It is a formidable challenge to monitor nanoparticles *in vivo*. Tedious *post-mortem* analysis of samples derived from various organs and tissues in combination with a large variety of detection methods (e.g. transmission electron microscopy, silver staining, and many others) are required to assess NPs quantities. These methods are neither comprehensive nor quantitative, given the limited resources and manpower available in an average research group. Frequently, only selected organs are tested for nanoparticle presence, resulting in an incomplete biodistribution picture. Still, these methods are used extensively for nanoparticle detection in biological samples. Non-invasive methods of detecting nanoparticles *in vivo* throughout a whole animal body involve such complex technologies as magnetic resonance imaging (MRI) and X-ray computer tomography (CT). Such methods present their own complications associated with high cost, availability of instrumentation, and the need for additional hazardous contrast agents. There is a definite need for improved and low-cost methods and instrumentation for non-invasive measurements of nanoparticle biodistribution.^{4,5}

In this work, we have used our three dimensional laser optoacoustic imaging system (LOIS-3D) described previously⁶⁻⁹ to track the dynamics of gold nanorod distribution in live mice. Optoacoustic imaging has been proven effective in imaging blood vessels and organs due to inherent differences in their optical absorptivities. Since gold nanorods are excellent absorbers of light at their plasmon resonance wavelengths, they can be detected with optoacoustic imaging system *in vivo* even in the presence of endogenous optoacoustic signals from organs and tissues. In our experiments, several mice injected with synthesized GNRs were imaged with LOIS-3D before and after injection. The presence of gold nanorods was detected as the localized changes of optoacoustic signals inside the mouse body. Tomographic images acquired at different time points revealed changes in organ and tissue absorptivities related to GNR accumulation and clearance. This demonstration highlights potential and versatility of optoacoustic imaging technology for non-invasive monitoring of nanoparticles in live organisms.

2. MATERIALS AND METHODS

2.1 Fabrication, Purification and PEGylation of Gold Nanorods

The GNR fabrication protocol was modified from a previously published paper on GNR production.^{3,10,11} The plasmon resonance of these high-yield GNR has a narrow band of rods around the 760 nm wavelength. Fabricating 100 mL solution of GNR would start with preparation a solution of seeds from 50 μ L of an aqueous 0.01 M solution of $\text{HAuCl}_4 \cdot 3\text{H}_2\text{O}$ added to 1.5 mL of a 0.1 M CTAB solution in a test tube and 120 μ L of an aqueous 0.01 M ice-cold NaBH_4 solution all at once. This solution was to be used within 2-4 hours after preparation. After this, the next step of fabrication is to get the exact proportions of 94.4 mL of 0.10 M CTAB, 3.96 mL of 0.01 M $\text{HAuCl}_4 \cdot 3\text{H}_2\text{O}$, and 0.60 mL of 0.01 M AgNO_3 solutions and add in that order, one by one. After they had been added sequentially, 0.64 mL of 0.10 M Ascorbic Acid was added and a wait period of about 10 minutes to allow for the reaction to fully complete. After this, 0.40 mL of seed solution was added and then this solution was kept at 30 $^\circ\text{C}$ for at least 12 hours. The GNR are then centrifuged at low speed of 3,000 rpm for 10 min for separation of other aggregates such as platelets and stars. This pellet is removed and following this, only the remaining supernatant fraction was used.

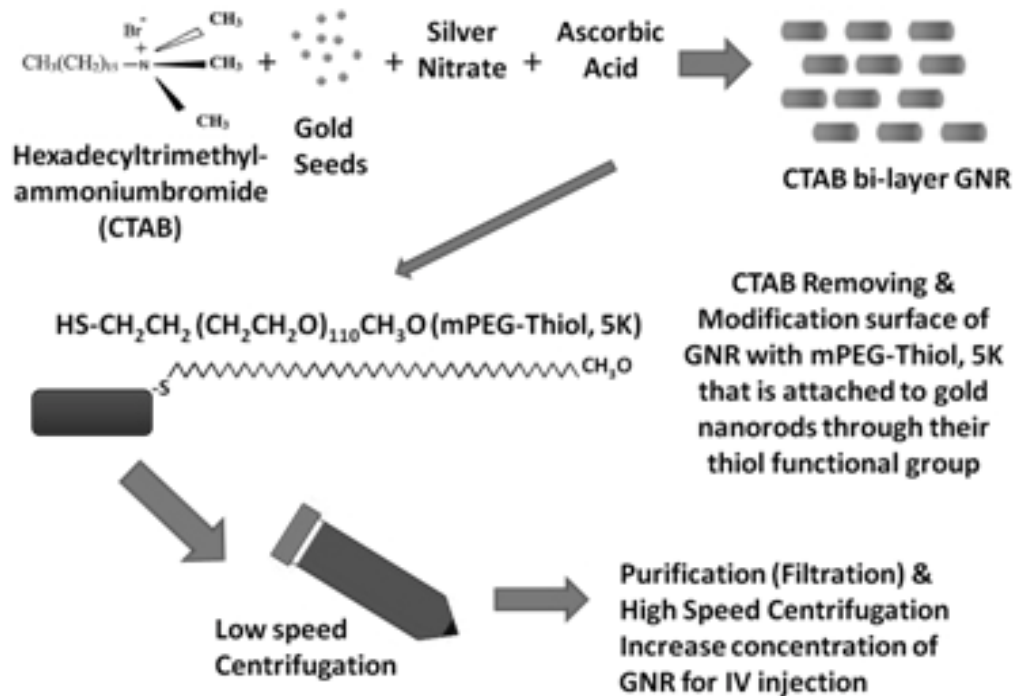


Figure 1 – Diagram of the synthesis and PEGylation of GNR production used in these experiments

In order for the PEGylation of the GNR solution, a previously established design was mimicked.^{12,13} After the GNR solution underwent low speed centrifugation, it was centrifuged again at 14,000 g for 10 minutes. The supernatant was discarded and the pellet resuspended in deionized water. 1.0 mL of 2 mM potassium carbonate (K_2CO_3) was added to 8 ml of aqueous GNR solution and 1.0 ml of 0.1 mM mPEG-Thiol-5000 (Laysan Bio Inc., Arab, AL). This resulting mixture was kept on a rocking platform at room temperature overnight. Excess mPEG thiol was removed from solution by two rounds of centrifugation and the final resuspension of the GNR-PEG was in PBS (pH 7.4). The GNR-PEG conjugate was filtered through a 0.22 μm Millipore Express Plus Membrane which it is important to note that the filtration does not change the properties of GNR. An increase in concentration of PEGylated GNR was made by centrifugation at 12,000 g for 10 minutes with the supernatant being removed and the pellet resuspended in PBS pH 7.4 up to a concentration of 12.5 nM (or an optical density around 50, measured from a Thermo Scientific Evolution 201 Spectrophotometer). All steps of the synthesis and PEGylation of GNR can be seen in Figure 1.

2.2 Mouse Optoacoustic Experiment

The data acquisition system consisted of an arc array of 64 piezo-composite elements with a focal length of 65mm and center frequency of 3.1 MHz (Imasonic SAS, France). A Quanta Systems laser (Solbiate Olona, Italy) tuned at 765 nm with an output pulse at 10 Hz was attached to a randomized fiber bundle that had four rectangular outputs directed at the sample as shown at Figure 2. The bundle outputs provide laser fluence of $\sim 1 \text{ mJ/cm}^2$ at the target. A custom made data acquisition system and amplifier capable of providing up to 90 dB of variable gain was set to a constant gain of 55 dB for the scans. The sampling frequency was done at 25 MHz over 1536 samples with an average of 32 acquisitions. Scans were done in a temperature-controlled water tank at a constant 36 °C. Sample rotation was performed with a computer controlled DC motor (Oriental Motors). Image of the experimental setup are shown in Figure 2. Mouse scans were performed using full 360° rotation in 2.4° steps for a total of 149 acquisitions. Additional details on the system hardware was described previously.^{6,8,9}

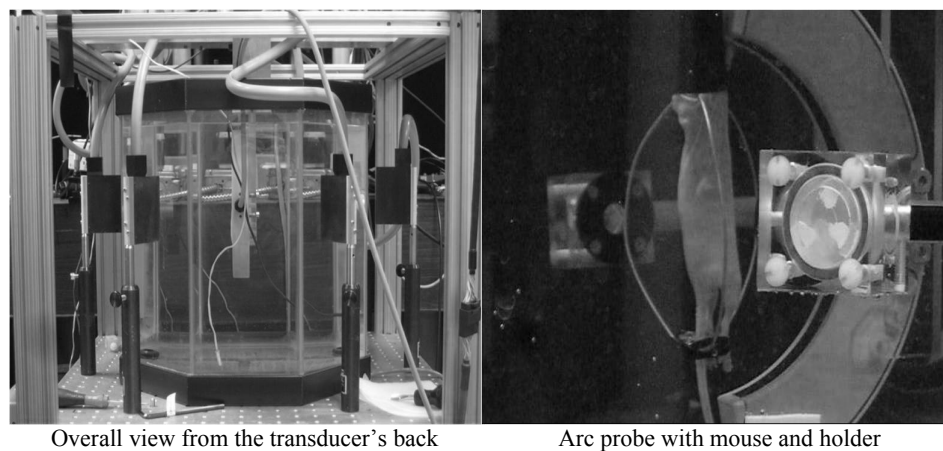


Figure 2 – Setup of the mouse scanning system with rectangular fiber bundles

Athymic Nude-Foxn1^{nu} mice (Harlan, Indianapolis, Indiana) were chosen for the experiments. Ages and weights of the animals were 7-9 weeks and 23-27 g, respectively. The mice were given isoflurane at 3% as an anesthesia agent. The anesthetized mouse was placed to a custom mouse holder. The head of the mouse was placed in a diving bell which supplied breathing gas (mixture of oxygen, air, and isoflurane). The mouse was transferred to the heated water tank, and the isoflurane was lowered to 2%. The mice were first scanned prior to injection to acquire reference images for comparison. Then, the mice were taken out of the tank and given intravenous (IV) injection of GNR-PEG solution. Optoacoustic scans were done either 1 hour after IV injection or 24 hours after. Another group of mice was given an IV injection but not scanned. The mice were sacrificed at 24, 72 and 192 h after the IV injections of GNR, and their liver were extracted. From these samples of liver, 5 μm -thick slices were prepared and stained with Silver Staining kit (BBI

International, UK) according to the manufacturer's instruction. Enhancement of GNR was assessed with optical microscopy. In every case, 400 μL in sterile PBS with concentration 7.5×10^{12} GNR /mL was injected.

Signal processing included signal deconvolution to account for the system transfer function and filtering up to seven scales of wavelets.¹⁴ Reconstruction was done by a custom designed 3D algorithm utilizing the filtered radial back projection method after the application of the signal deconvolution and integrated wavelets. Due to the arc shape and object rotation, there is a higher density of transducers at the poles of the sphere of transducers but are weighted accordingly to ensure equal contributions of signal samples to each voxel of the reconstruction globe.⁸ The parameters related to image processing were identical in every case to allow their quantitative comparison.

3. RESULTS & DISCUSSION

As-synthesized GNR samples are purified with centrifugation to achieve better homogeneity of the sample for *in vivo* applications. The results of centrifugation can be seen in Figure 3. One can see that centrifugation is needed to purify samples impurities that do not absorb at the wavelength of interest. GNR samples exhibit strong and narrow optical resonances around 760 nm that matches the biological transparency window.^{3,15} The observed stability of GNR-PEG on the timescale of several months was similar to reports from other groups.¹⁵⁻¹⁷

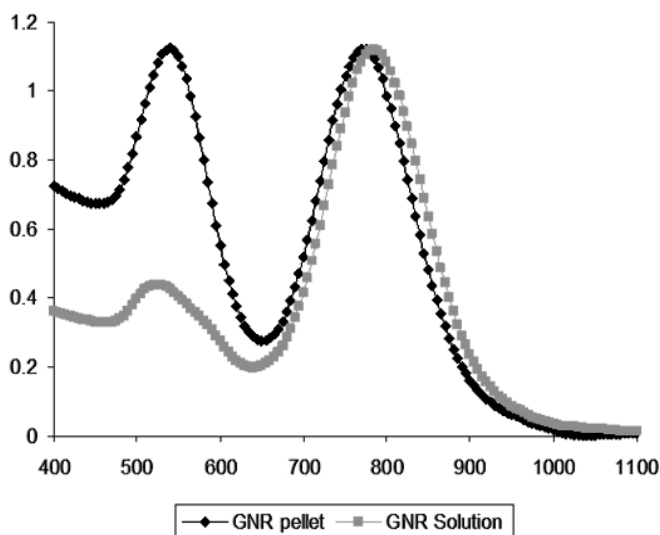


Figure 3 – Spectra of GNR at different after centrifugation comparing pellet to solution

The upper images in Fig. 4 show three-dimensional optoacoustic reconstructions from the scans taken from the rotational tomography system with a voxel resolution of 0.1 mm. The transparency is based on gradients where a more opaque object has higher gradient when compared to its neighboring voxels which are then more transparent. Image settings were held constant to see qualitative differences from before GNR injection (control) versus after GNR injection after an hour and around 24 hours in essence normalizing the images' brightness from black to white. Due to the normalized image spectra between the three scans, the pre-GNR injection is seen as rather dim and dark. In its corresponding zoomed image of the left kidney and spleen, one can see faintly the kidney and spleen but they are neither the brightest nor the most opaque object. After an hour post-GNR injection the spleen and kidneys do become slightly brighter but it is not the only thing that is seen brighter. The peripheral blood vessels around the back, ribs, and underneath the arms are seen much brighter than before and are the brightest and most contrasted objects now. This is quite apparent in the zoomed in area of the left kidney and spleen especially when compared to prior GNR injection. After 24 hours, the periphery blood vessels that were once so visible are now almost gone and instead the kidneys, spleen, and liver are now the brightest. The spleen specifically looks to be the most contrasted as it be quite opaque and the brightest overall as well. The vertebrae interestingly enough are also quite apparent during this time. The lower three images of Figure 4

show a zoomed image of the left side of the mouse cropped to the region of the left kidney and spleen with parts of the spinal cord with further magnification so that one can compare the left kidney and spleen to one another more easily. It can also be seen there that it is indeed that various vertebrae discs of the mouse being visualized.

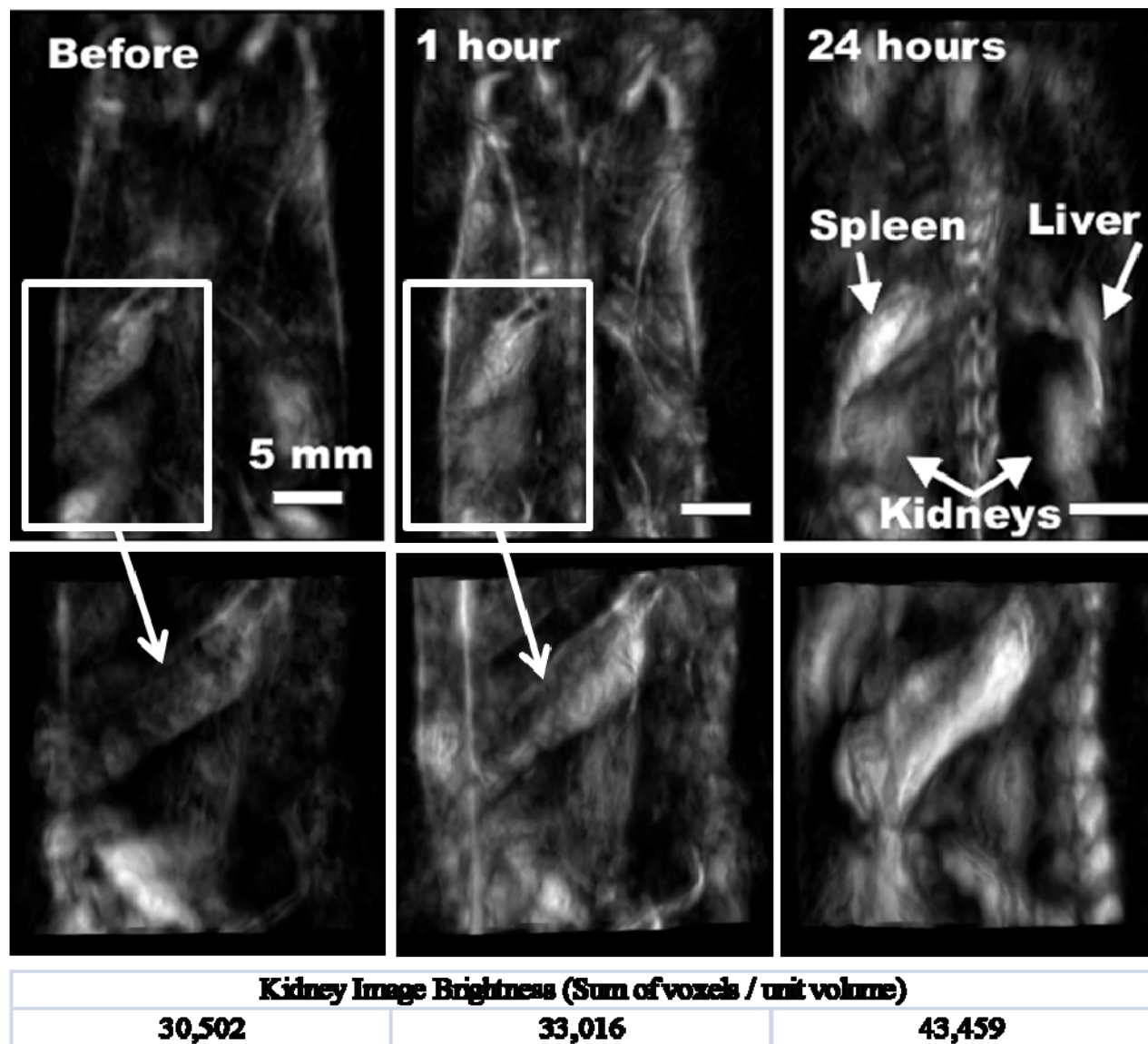


Figure 4 – Volumetric screenshots cropped onto the back of the mice to show the kidneys and spleen

A small table can be seen at the bottom of Figure 4 which displays a summation of voxel brightness within the various times of the scans. Optoacoustic slices were taken off of the central region of the left kidney optoacoustic image with dimensions of 6×4 mm up to 1 mm and summed. In terms of voxel brightness, if the prior to GNR injection were taken as the base/control then after an hour there is only an 8% increase in brightness followed by a more significant 42% increase in brightness after 24 hours. These results would mean that nonspecific GNR were not accumulating within the kidney after an hour post-GNR injection. After a day however a significant increase in image brightness can be found within the kidneys as compared to pre-GNR injection which leads to the belief that GNR are accumulating within certain organs such as the kidneys, liver, and spleen following a day in the circulatory system of the mice. The 8% increase can

be attributed to the GNR still being distributed throughout the body of the mouse and in the blood vessels near by the kidneys. A 42% increase in image brightness though is quite significant and shows promise in possibly the ability to distinguish to some extent the number of GNR at the site or at least serve as a confirmation that the optoacoustic contrast agent arrived to the site as expected once they are targeted GNR.

We know, that the strong light extinction (absorption and scattering) of gold nanorods has been employed in various biomedical imaging applications.¹⁸⁻²⁰ Slices of excised liver tissue were taken from another set of mice to track the accumulation of GNR as well as possible toxicity effects in liver tissue over a span of eight days which are displayed in Figure 5. Within the silver staining images, it is seen that from a day up to three days there is a visible increase of GNR within the liver. After eight days though, this accumulation looks to decrease from the liver. The silver staining image of a day and three days show that the optoacoustic image's increase in brightness is likely due to the accumulation of GNR within the spleen, kidney, and liver. We investigated with hematoxylin and eosin staining which showed no visible differences between the PBS control and the GNR slices. As we know the hepatotoxicity (liver damage) occurs because of the accumulation of nanomaterials in the liver (and spleen) are being taken up by the reticuloendothelial system (part of the immune system where complex components communicate to identify, capture, and filter foreign antigens and particulates) which could lead to hepatotoxicity.^{18,21} Looking at Figure 5d (8 days) to Figure 5c (3 days) there is a decrease in GNR seen in the liver therefore the toxicity of the fabricated GNR which were injected intravenously in the mice is determined to be minimal. However, Cho et al.²² studied the toxicity of 13 nm PEG modified gold nanoparticles in mice (4.26 mg gold/kg) and found that the nanoparticles accumulate in the liver 168 h after injection, and induce acute inflammation and cellular damage in the mouse liver. We used 20 mg/kg body mass PEG modified GNR and did not find any significant morphological damage of any consequence in the liver of mice. This is credible witness that after our purification of PEGylated GNR is not toxic for mice.

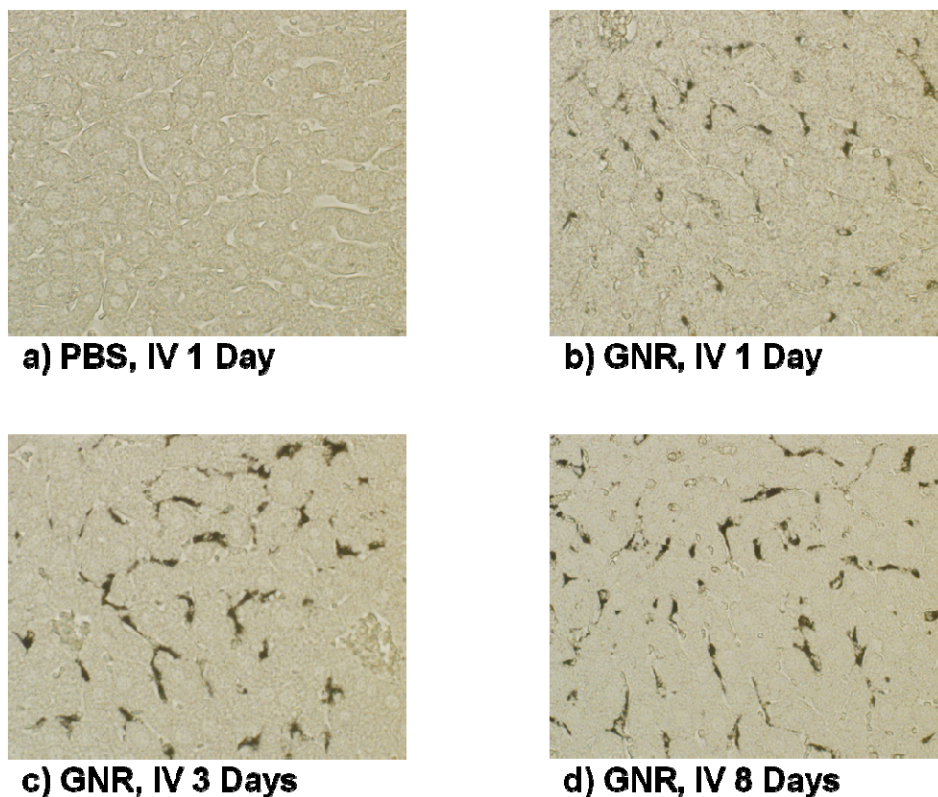


Figure 5 – Silver staining of PEGylated gold nanorod (GNR) accumulation in mouse liver following intravenous (IV) injection

4. CONCLUSION

GNR distribute themselves within the circulatory system of mice within an hour or two and provide large contrast within the peripheral circulatory system of the mouse but during such time much of the GNR do not end up in the organs of the mice. After a day there is a definite increase in GNR accumulation in certain organs such as the kidneys, spleen, and liver. This is seen in our findings with optoacoustic imaging, as within an hour the GNR are still within the circulatory system. After a day post-GNR injection, the GNR accumulate within certain organs such as the spleen, liver, and kidneys. Excised liver tissue, which underwent silver staining to see GNR distribution, show a maximum at 2-3 days after GNR administration. The toxicity of the fabricated and purified PEG modified GNR which were injected intravenously in the mice is determined to be minimal or nontoxic for rodents. It is demonstrated here that there are significant changes in image brightness which shows considerable promise that optoacoustic imaging can track the distribution of untargeted and targeted GNR. Our data shows that it is possible to track intravenously administered GNR as contrast agents that will increase the resolution of optoacoustic imaging over extended periods of time without dangerous consequences.

5. REFERENCES

- [1] J.A. Copland, M. Eghtedari, V.L. Popov, N. Kotov, N. Mamedova, M. Motamedi, A.A. Oraevsky, "Bioconjugated gold nanoparticles as a molecular based contrast agent: Implications for imaging of deep tumors using optoacoustic tomography", *Molecular Imaging and Biology* 2004 6(5), 341-349 (2004).
- [2] Ferrari M., "Cancer nanotechnology: Opportunities and challenges", *Nature Reviews Cancer* 5(3), 161-71 (2005).
- [3] Oraevsky A. A., "Gold and silver nanoparticles as contrast agents for optoacoustic imaging", [Photoacoustic imaging and spectroscopy, 1st ed.], Taylor and Francis Group, New York, Chapter 30 (2008).
- [4] Thomas T, Bahadori T, Savage N, Thomas K., "Moving toward exposure and risk evaluation of nanomaterials: challenges and future directions", *Wiley Interdisciplinary Reviews-Nanomedicine and Nanobiotechnology* 1(4), 426-33 (2009)
- [5] Riehemann K, Schneider SW, Luger TA, Godin B, Ferrari M, Fuchs H., "Nanomedicine-Challenge and Perspectives", *Angewandte Chemie-International Edition* 48(5), 872-97 (2009)
- [6] Fronheiser M.P., Stein A., Herzog D., Thompson S., Liopo A., Eghtedari M, Motamedi M., Ermilov S., Conjusteau A., Gharieb R., Lacewell R., Miller T., Mehta K, Oraevsky A.A., "Optoacoustic System for 3D Functional and Molecular Imaging in Nude Mice", *Proc. of SPIE* 6856, (2008).
- [7] Brecht H.P., Su R., Fronheiser M., Ermilov S.A., Conjusteau A., Liopo A., Motamedi M., Oraevsky A.A., "Optoacoustic 3D Whole-Body Tomography: Experiments in Nude Mice", *Proc. of SPIE* 7177, (2009).
- [8] Brecht HP, Su R, Fronheiser M., Ermilov S. A., Conjusteau A., Oraevsky A. A., "Whole Body Three-Dimensional Optoacoustic Tomography System for Small Animals", *J. Biomed. Opt* 14(06), 064007, (2009).
- [9] R. Su, H.-P. Brecht, S. A. Ermilov, V. Nadvoretzky, A. Conjusteau, A. A. Oraevsky, "Towards Functional Imaging using the optoacoustic 3D whole-body tomography system", *Proc. of SPIE* 7564, (2010).
- [10] Sau TK, Murphy CJ. "Seeded High Yield Synthesis of Short Au Nanorods in Aqueous Solution", *Langmuir* 20, 6414-6420 (2004).
- [11] Eghtedari M, Oraevsky AA, Copland JA, Kotov NA, Conjusteau A, Motamedi M. "High sensitivity of in vivo detection of gold nanorods using a laser optoacoustic imaging system", *Nano letters* 7(7), 1914-8 (2007).
- [12] Eghtedari M, Liopo AV, Copland JA, Oraevsky AA, Motamedi M. "Engineering of Hetero-Functional Gold Nanorods for the in vivo Molecular Targeting of Breast Cancer Cells", *Nano letters* 9(1), 287-91 (2009).
- [13] Niidome, T., Yamagata, M., Okamoto, Y., Akiyama, Y., Takahashi, H. and Kawano, T., "PEG-modified gold nanorods with a stealth character for in vivo applications", *Journal of Controlled Release* 114(3), 343-347 (2006).
- [14] Conjusteau A, Ermilov SA, Brecht HP, Oraevsky AA, "Effects of optical energy distribution on the generation of acoustic plane waves", *Proc. Of SPIE* 7564, (2010).
- [15] Alkilany A. M., Murphy C. J. "Toxicity and cellular uptake of gold nanoparticles: what we have learned so far?", *J Nanopart Res* 12, 2313-2333 (2010).
- [16] Liao H., Hafner J. "Gold Nanorod Bioconjugates", *Chem. Mater* 17, 4636-4641 (2005).
- [17] Huang XH, El Sayed IH, Qian W, El Sayed MA. "Cancer cell imaging and photothermal therapy in the near-infrared region by using gold nanorods", *Journal of the American Chemical Society* 128(6), 2115-20 (2006).

- [18] Dobrovolskaia MA, McNeil SE. “Immunological properties of engineered nanomaterials”, *Nat Nanotechnol* 2, 469–478 (2007).
- [19] Stone JW, Sisco PN, Goldsmith EC, Baxter SC, Murphy CJ “Using gold nanorods to probe cell-induced collagen deformation”, *Nano Lett* 7, 116–119 (2007).
- [20] Cho EC, Xie JW, Wurm PA, Xia YN “Understanding the role of surface charges in cellular adsorption versus internalization by selectively removing gold nanoparticles on the cell surface with a I2/KI etchant”, *Nano Lett*, 9, 1080–1084 (2009).
- [21] Chen YS, Hung YC, Liao I, Huang GS “Assessment of the in vivo toxicity of gold nanoparticles”, *Nanoscale Res Lett*, 4, 858–864 (2009).
- [22] Cho WS, Cho MJ, Jeong J, Choi M, Cho HY, Han BS, Kim HS, Kim HO, Lim YT, Chung BH “Acute toxicity and pharmacokinetics of 13 nm-sized PEG-coated gold nanoparticles”, *Toxicol Appl Pharmacol* 236, 16–24 (2009).